IMPACT OF POLYMERIC CHANGES ON MECHANICAL AND STRUCTURAL PROPERTIES OF POLYETHYLENE SELF REINFORCED POLYMER COMPOSITES

Deepa A[1], Kuppan P[2], Padmanabhan K[3]

The present study addresses the mechanical behavior of polyethylene self-reinforced composites (SRC's) considering polymeric structural changes after cutting. Self-reinforced polyethylene composite is fabricated using the HOT compaction method by maintaining the processing temperature at 160 ˚C. Conventional and unconventional methods were used to cut the samples of standard dimensions. FTIR images revealed the formation of C=C, C-N, N-H bend bonds after laser cutting, initiated a decrease in the surface roughness value to 4.68µm (Ra).SEM analysis is performed to analyse the structural integrity and damage failure of SRC's. Structural changes formation after Laser cutting leads to improve the ultimate tensile strength of the laminate ~ 20% compared to Conventional cut samples. Similar trend is noticed for flexural properties and Shore –D hardness values of the SRC composite laminate correlated to polymeric changes with conventional cutting due to the formation of C-N bond but less UTS is observed compared to laser cutting.

Keywords: Polymeric changes; Mechanical properties; Structural properties; Polyethylene SRC Composites,

1. Introduction

1.1 Background and Manufacturing of SRC's

Polymer composites are lightweight thermoplastic materials with low density, unique chemical properties and cross-linkages. Recently, polyethylene self-reinforced composites (SRC) of highly oriented crystalline fiber and matrix have been developed. Polyethylene self-reinforced composites are considered because of its lightweight and effective mechanical characteristics [1]. Also, polyethylene SRC composites reinforced fiber and matrix belong to the same family of thermoplastic polymer, which can be recycled. Polyethylene SRC laminate can be developed and held strongly which allows the polyethylene SRC laminate to achieve high tensile resistance, excellent insulation properties, cost-effective correlated to GFRP or CFRP laminates. However crystalline fibers have a significant effect on mechanical properties which are extremely affected by the fabrication process [2]. Hence, many researchers reported characterization based on the manufacturing process. Processing of thermoplastics is easy because of high decomposition temperature during the HOT compaction process. The fabrication process affects the mechanical

[1], [2,3] SMEC, Vellore Institute of Technology, Vellore-632014, deepa.a@vit.ac.in

properties and physical properties of the composite [3]. The mechanical properties of SRC composite can be enhanced using thermal treatment and extrusion processes. With a growing interest in SRC's effective processing technique is required. Researchers reported that high- performance SRC's can be processed using HOT composition method with suitable processing temperatures [4].

1.2 Advanced Machining of SRC's

With the increased use of polymer composites in automotive, naval, electronics, aerospace respectively and optimization of machining parameters for SRC's has become more important. The machining of SRC laminates also becomes a necessity to protect the structural and mechanical properties of composites [5]. Conventional machining processes like drilling, end milling, turning and planing have been applied to self-reinforced composite laminates to study its impact on structural integrity. Implicit anisotropy and heterogeneity of composite material during conventional machining contributes to the failure of composites due to matrix fracture, fiber pull out, delamination, etc. Minimization of cutting inferred damage becomes an important factor due to the structural coherence of composites [6].

Machining with an improved surface quality finish of laminate has been narrated with advanced machining techniques like laser machining and Abrasive water jet machining (AWJ) [7]. The nature of absorbing moisture by most of the fibers and polymers affects the molecular structure of thermoplastic composite through the degradation process. The probability of abrasive particle detainment in the laminate contributes to a decrease in strength after AWJ machining [8]. Laser machining has growing attention as a result of dry machining and the non-contact type tool used during machining over traditional machining. Many researchers have optimized machining parameters for the non- conventional machining of FRP's to get the best results [9]. The research inferred that low power and high scan speed can reduce delamination while laser machining. Distinct studies were done to reduce heat affected zones and thermal damage developed during advanced machining [10]. Major problems recognized are surface damage, delamination, and thermal instability. The temperatures observed during laser cutting result in structural fracture, machining damage, especially the heat- affected area [11]. The temperature generated while laser machining originates to matrix degradation of self-reinforced polymer laminate develops the ductility of the matrix. The variation in conduction properties between polymers and fibers results in uneven surfaces during laser machining [12]. Studies on Kevlar-polyethylene laminates machined using laser machining reported that HAZ followed an increasing trend between 0.75 to 1.7mm at the entrance and 0.8 to 1.5mm at the exit. The damage factor of Kevlar polypropylene and Kevlar polyethylene laminates is ~ 1.2 for all input energies.

SEM images reported that K-PE samples matrix failure is faster compared to K-PP. Studies have been carried out to reduce thermal damage and heat-affected zones developed during non-conventional machining [8-9]. Li et al. used NDYAG laser (355nm) to drill carbon fibre reinforced fibres and optimized the laser machining parameters to reduce the HAZ/damage zone. Li et al. suggested shorter wavelengths to cut CFRP samples to minimize HAZ. Riverio et al. found that 540µm HAZ is observed using 3.5kW of laser power. Hejjaji et al. found that surface roughness of laser machined laminates is high than the conventionally machined sample.

1.3 Present State of Knowledge in advanced Machining

Advanced machining techniques improvement in Structural properties of composites is quite successful for a wide variety of fiber composites including GFRP, Kevlar and CFRP laminates. AWJ machining and laser machining study on thermoset based composites are studied but thermos-plastic based laminates machining is lagging. Different loading parameters influence the chemical structure, morphology and thermo-mechanical properties of the SRC's [13-15].

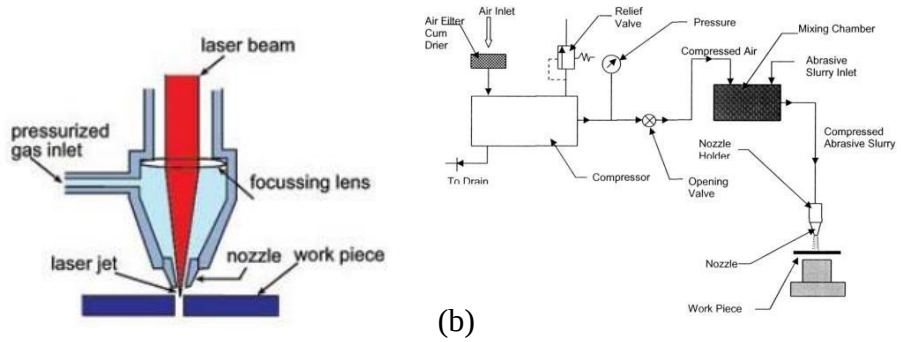

(a) (b)

Fig 1. Diagrammatic representation of (a) Laser cutting process (b) AWJ machining

CO_2 laser machining shown in Fig.1 (a) is used to reduce the electrical resistivity of PE/MNWT composite. An increase in the content of MWCNT leads to a reduction in electrical resistivity. FESEM reveals the effect of laser parameters on resistivity of Polyethylene composite.HAZ values ranged between 0.75-1.7 mm and are at the entrance and 0.8 to 1.5 mm at outline is observed with an increase in line energy [16]. AWJT process shown in Fig.1 (b) is a better machining method for LPDE material than the conventional machining methods. Minimum ASR of 1.67 lm and maximum MRR 14072.02 mm3/min were obtained respectively; at optimum parameters of 5 mm/min nozzle feed rate, 350 g/ min abrasive flow rate and 2500 min–1 spindle speed [8].

This work gives a detailed investigation about machining induced damage of self-reinforced composites (SRC) in conventional and non-conventional machining. The effect is characterized by studying surface morphology using scanning electron microscopy. Aspect ratio, the functional group, and Structural

integrity are studied using FT-IR Spectroscopy, DSC and Thermogravimetric analysis (TGA) [18-21]. In addition tensile tests (ASTM D 638) [22], Flexural test (ASTM D 790M), Hardness test (Shore D) were implemented to determine elastic properties and hardness of the Polypropylene SRC [23].

2. Experimental setup and measurement procedure

2.1. Experimental Procedure

The entire fabrication process is shown in Fig.2. The Raw Materials like Polyethylene- polyethylene Terephthalate (PE-PET) fabric plain weave and HDPE- high-density polyethylene matrix sheet of 1mm thickness (Korea E&T Co.Ltd) were used to prepare the laminates. The Polyethylene fabric shown in Fig.2 was used to fabricate the laminates under a consolidated temperature. Differential Scanning calorimeter (DSC) (SDT Q600 V20.9 Build 20, USA) was used to acquire the thermal stability (consolidated temperature) of the fibres and matrix samples. Initial temperature, residual mass and thermal stability were determined using TGA.

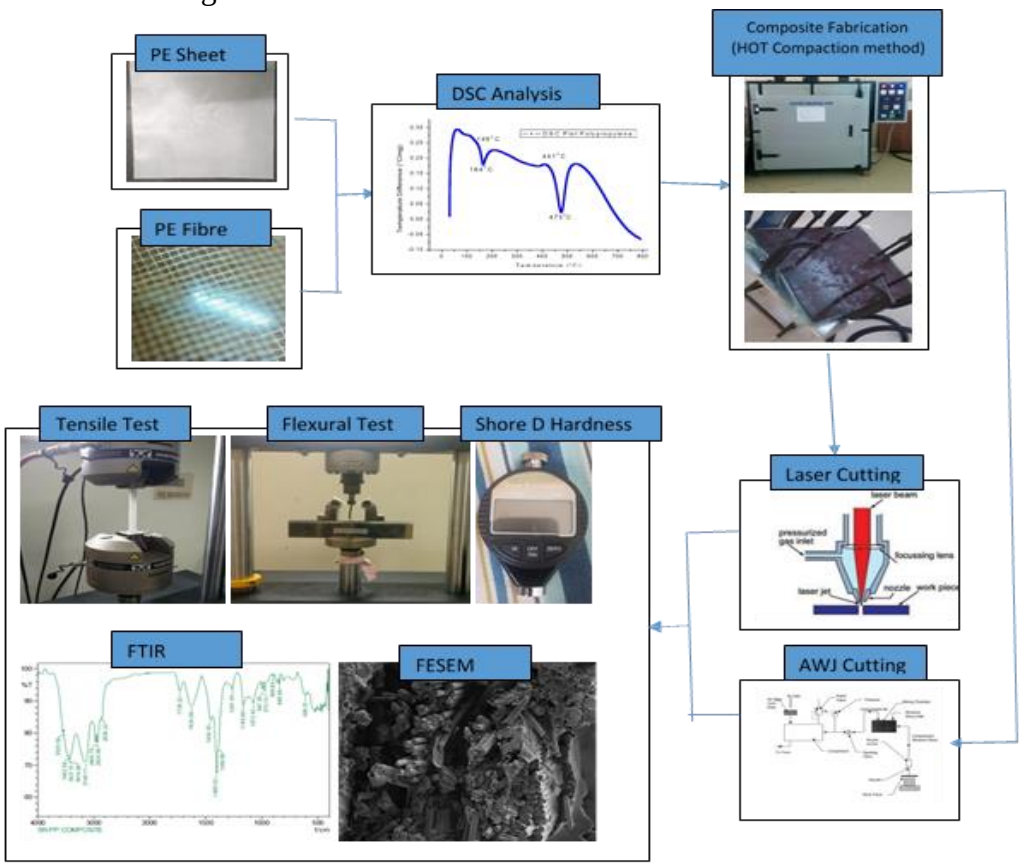

Fig.2.Experimental Procedure

An analysis was implemented initially with fibre and matrix of few milligrams at elevated thermal environments from 20 to 600 degrees and DSC analysis was also carried out at the same environmental conditions. The softening temperature determined from the DSC plot is used to fabricate SRC composite using HOT compaction method.

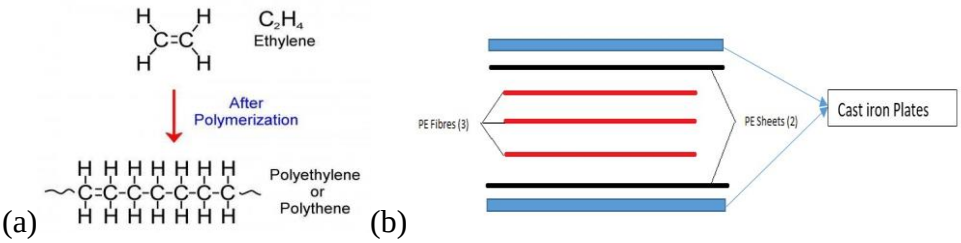

Fig .3. (a)Polymeric structure of Polyethylene **(b)** Schematic diagram of Fibre lay up of HOT Compaction method

The laminate is prepared using three polyethylene fibers and two high-density polyethylene matrix of size 500mm×500mm. The polyethylene fiber and HDPE matrix arrangement were as shown in Fig. 3(b) were processed at 160^{O}C in the oven and then cooled down for one hour. The processing temperature for the Hot-compaction method was measured using Differential scanning calorimetry (DSC) curve shown in Fig.4. A CO_2 Laser cutting machine (AMADA LCG 3015, India) was used to cut the samples. A Laser head speed of 420mm/min, laser nozzle diameter size of 1.7mm and a standoff distance between the laser nozzle and the composite laminates surface of 15mm, was maintained. The work table was CNC controlled with the focal length of the lenses at 200mm. A chiller unit was used to cool down the laser head and the laser source. The work area was enclosed by sliding doors. The fabricated laminates were also cut using an abrasive water jet machining system (OMAX 3030) where the abrasive particle flow rate of 800 g/min was maintained to cut the Polyethylene SRC samples. The feed rate of the water jet was 1500m/s. The stand-off distance was 4mm between the surface and the nozzle. The water jet pressure of the system was maintained at 4000 bar.

2.2. Measurement procedures

The dimensions of the tensile specimens cut using conventionally and unconventionally cutting were 250mm×25mm×2mm based on the standard ASTM D 638. The analysis was implemented with a loading speed rate of 2mm/min using a universal testing machine (Instron 8801). The dimension of the flexural specimen was 125mm×25mm×2mm based on the standard for flexure ASTM D 790 M. The flexural test was carried out in the same Instron machine at a support span length to thickness ratio of 16:1. The loading rate of the central crosshead was 2 mm/min.

Shore D Hardness Test was performed using Durometer (GIANT 14876) which measures the depth of a depression developed by a force utilizing regulated presser foot on the sample. This depth is reliant on the shape of the presser foot, Visco and elastic properties, the hardness of the material. ASTM D2240 durometers are allowed to measure the primary hardness of the sample and concluding hardness after a duration of time [24, 25]. By applying the consistent force, without shock, hardness (depth of indentation) can be measured. Force is applied for timed hardness up till the required time and then interpret. The thickness of the material used for this analysis is 6.4 mm (0.25 inches).

3. Results and discussion

3.1. DSC and TGA analysis of Polyethylene

The thermal stability of polyethylene fiber and matrix is investigated performing DSC and TGA analysis. Peaks shifted for polyethylene are as shown in Fig.4. DSC curves of Polyethylene obtained during the second stage of the process of heating are represented in Fig 4. (a). Transformations comprised of DSC plot were observed and interpreted, change in enthalpy related to change of material from glassy is around 60 °C, exothermic solidification at 90 °C, polymer matrix softening at 136°C and level of crystallinity is 50% as shown in Fig.4.

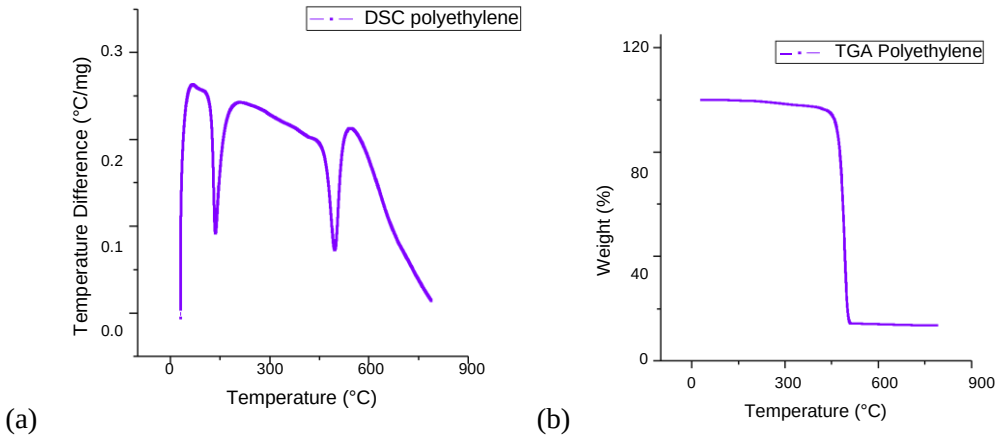

Fig .4. (a) DSC plot of Polyethylene (b) TGA plot of Polyethylene

The TGA plot of Polyethylene exhibits density loss contour at distinct temperatures, as represented in Fig.4 (b). The initial level of density loss was observed at a range of temperatures around 30–175 ◦C, in representation with a weight loss of 7% of moisture. A non-oxidative thermal degradation occurred

under nitrogen flow in polyethylene, which was identified at a temperature range of 200–480 ◦C signifies the de-propagation till the end of the Polyethylene chain.

The chemical changes at the initial debonding stage of the Polyethylene chain lead to evaporation and elimination of explosive products. The deterioration of Polyethylene is increased beyond 300 oC lead to the development of a cyclic and crosslinked design. The deterioration of Polyethylene is increased beyond 300 ^{o}C lead to the development of cyclic and cross-linked chains. Further degradation leads to the formation of methyl ester and alkyl free radicals. A carbonize develops after 480 $^{\circ}$C and decay occurred at around 620 ◦C, remaining debris of around 1.3% w/w at the thermal condition of 750 ◦C.

3.2. Effect of structural change on tensile strength

The influence of structural integrity due to cutting on the Tensile strength of polyethylene SRC laminate is illustrated in Fig.5. The Ultimate tensile strength (UTS) of Polyethylene SRC laminates increased after advanced cutting by ~20%. This increase in tensile strength shown in Fig.5 (b) and Fig.5(c) is probably because of the chemical changes that occurred after advanced cutting, continuous depreciation of the hydrates, which contribute enhancement in tensile characteristics of the laminate. Moreover, this increasing inclination in tensile strength also results from enhancing plasticity and adhesion between the fiber and matrix due to advanced cutting. Because of the formation of N-H, C-N, C==C, Acyl bonds after advanced cutting the tensile and flexural strengths of the polyethylene composite exhibit an improvement.

From Fig.5 the laser cut polyethylene samples have a higher load-bearing capacity compared to conventionally cut samples. In the case of ultimate tensile strength, the laser cut samples exhibit a higher value than a conventionally cut sample because of the definition of the damage, cut and brittleness of the fiber. A similar trend is followed in the young's modulus. The AWJ cut samples experienced less surface cut damage compared to the laser cut samples. It is observed that the maximum tensile load and ultimate tensile strength of conventional samples are 1302 N and 25 MPa respectively. After laser cutting, the ultimate tensile strength is increased to 30 MPa due to the formation of C-N bonds which exhibit strong stretching and increased ductility compared to conventional samples. As the ductility of the sample is increased after Laser cutting, which causes for formation of stiff C=C double bond that exhibits an increase in the tensile load compared to laser cutting, thereby achieving a tensile strength of 30 MPa. C=C double bonds are stronger than C-N single bonds as the bond energy of the former is 612 KJ/mol and that of the later is 315 KJ/mol. The

extent to which these bonds are formed also contributes to the strength.

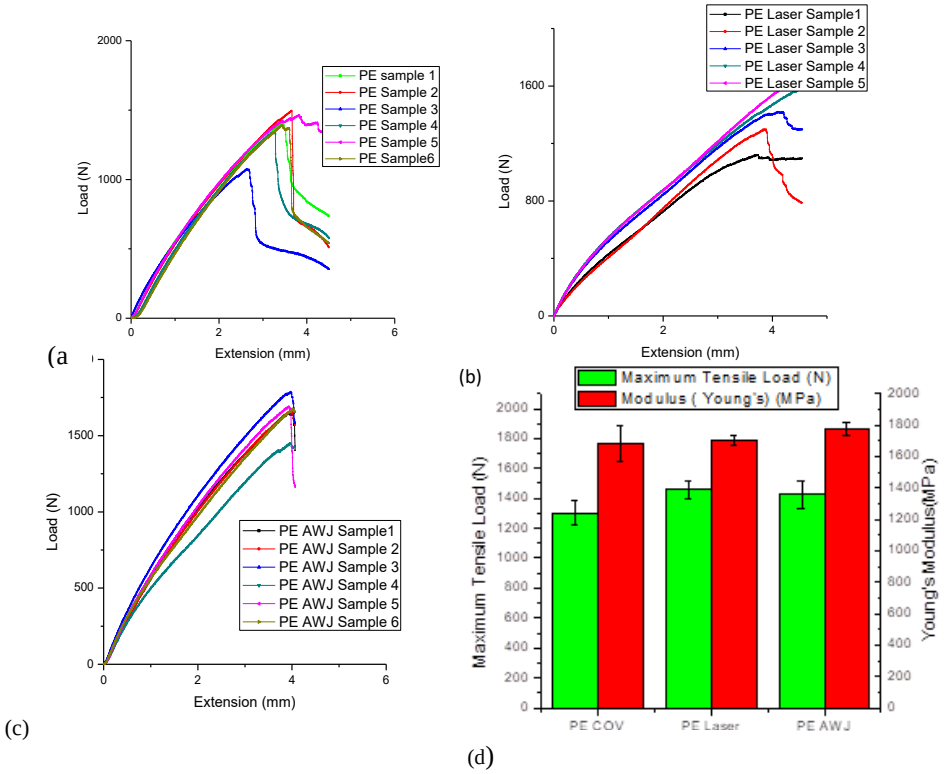

Fig .5. Tensile load plots of PE (a) Conventionally cut samples (b) laser-cut samples (c) AWJ cut samples (d) Average modulus and load plots

3.3 Effect of structural change on tensile modulus

The tensile modulus of the polyethylene composite varied because of the formation of change in the polymeric structure of composite after cutting. The effects of structural change on Young's modulus is shown in Fig. 5 (d). Increase of Young's modulus after advanced cutting from 1765 MPa to 1859 MPa is observed, this sudden increase is due to the formation of strong covalent bonds and N-H, Acyl, C=C bonds after cutting.

3.4. Effect of structural change on Ductility

Fiber ductility is increased after laser cut samples, the adhesion and debonding that occurs during conventional cutting are enhanced after laser machining which increases the strength of the composite. The effect of Structural change on ductility is shown in Fig.6.It is observed that ductility of polyethylene self-reinforced composite exhibit decrease after AWJ cutting from 1.12% to 0.7%.the laser cut sample exhibit an increase in ductility from 1.12% to 3.1%.

3.5. Effect of structural change on Ductility

Fig.6 (a) infers that the flexural strength of the laser cut samples is high compared to conventional machining by 21%. The N-H bend, aromatic and nitro bonds formation after advanced cutting is the reason behind the increase in flexural stress of the Polyethylene SRC laminate.

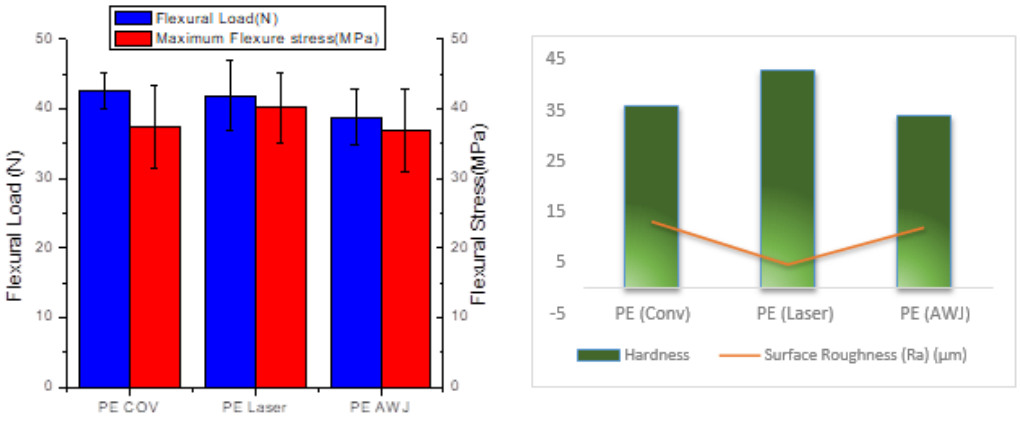

(a) (b)

Fig.6. (a) Flexural stress and load plots (b) Hardness values of Polyethylene SRC laminate for different machining parameters

The flexural stress and load-bearing capacity of laser cut samples are higher at 42 Mpa and 40 N respectively because of the formation of N-H Bend, C-O bonds and C-N bonds exhibiting a brittleness and stiffness in the sample as shown in the Fig.6. Flexural strength of the abrasive water jet cut samples was also high compared to conventional cut samples as a result of the formation of C=C bonds as shown in Fig.6(a).

3.6. Effect of structural change on Hardness and Surface Roughness

The surface roughness values after advanced cutting are less compared to conventional cutting as illustrated in Table 1, because of the increase in ductility of the composite after advanced cutting. The surface roughness (R_a) value of the laser-cut sample is decreased from 13.2 µm to 4.68 µm. A similar trend is shown for hardness in Fig.6 (b), Hardness value after laser machining increased from 34 to 43. Better mechanical properties with the smoother surface finish are observed in AWJ cut samples. Quenching after laser cutting plays a major role in improving the mechanical properties of the laminates.

Table 1. **Surface roughness measurements of Polyethylene (PE) Sample**

Sample Name	**$R_{A(\mu m)}$**	**$R_{q(\mu m)}$**	**$R_{z(\mu m)}$**	**$R_{max(\mu m)}$**	**$R_{p(\mu m)}$**	**$R_{v(\mu m)}$**	**Hardness (ShoreD)**
PE(Conv)	13.2	17.6	71	118	63	32	34
PE(Laser)	4.68	10.55	34.69	90.44	57	13	43
PE(Awj)	12.01	15.4	17.8	82.47	34	39	36

4. FTIR Spectroscopy Analysis

Spectral analysis comparison using FT-IR spectroscopy of Polyethylene SRC laminate originated for conventional cut, laser-cut and abrasive water jet cut are shown in Fig. 7 and Fig. 8. The band originated around 1080 cm^{-1} assigned for the ether compound is missing in the laser cut polyethylene SRC laminate, but the peak gradually appeared as the laminate is cut using AWJ jet cutting as inferred from Fig. 8(b). The absorption spectrum at 1467.15 cm^{-1} is the typical peak of Polyethylene SRC laminate which denotes the C-H bend Alkane group during advanced cutting is not visible in conventional cut spectrum. After laser cut of polyethylene samples, weak aldehydes, acid groups and ethers transformed to alkenes and N-H bend bonds, No ethers bond is found after laser cutting. Alkoxy, acyl, N=C groups are formed after AWJ cutting, which increases the strength of the composites.

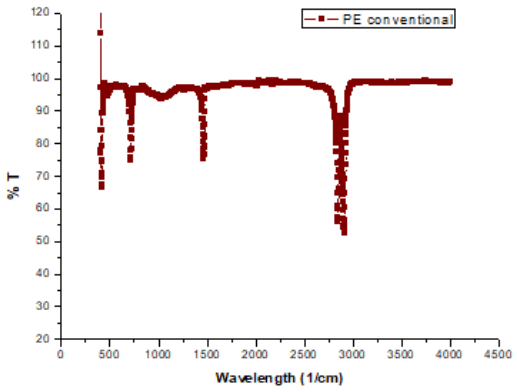

Fig. 7. FTIR Plot of PE Conventional cut sample

The absorption spectrum at 1165cm^{-1} is the–C–N stretching vibration observed after laser cutting due to reaction in open-air during cutting as seen in Fig .8(a). The spectrum around 1467.40 cm^{-1} characterized by the bending oscillation exhibited by the covalent (C–H) chain of the methyl group. Spectra at 2914cm^{-1} and 2846 cm^{-1} attribute to the acyl, N=C groups, C-O aromatic ester

and N-O stretching. An absorption band of 717 cm^{-1} is visible after AWJ cutting shows an alkene group that exhibits strong stretching and bending vibration. The C-C bonds have been converted into different bonds like C=C, C=O, C-F and C-N after laser cutting. The resultant bonds exhibit greater strength and stiffness than the C-C single bonds that existed before advanced laser cutting.

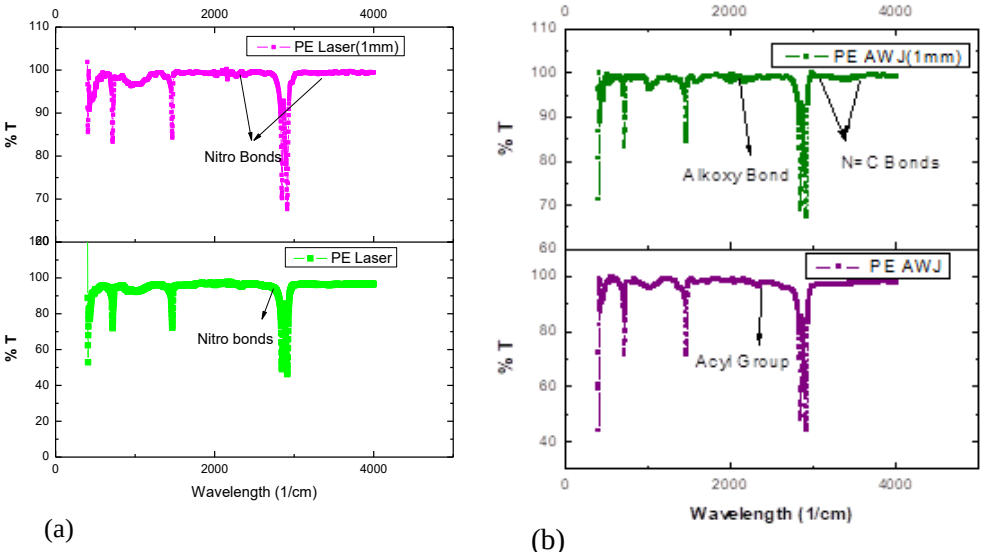

Fig. 8. FTIR Images of PE (a) laser sample (b) AWJ cut sample

The C=C bonds and the C=O bonds are more than twice as strong as carbon-carbon single bonds which can be the appropriate reason for an increase in the mechanical properties. All the samples exhibit similar spectra after ~ 1 mm of case depth. Chemical interaction and reaction occur only up to ~1mm thickness as depicted in Fig.8. A cross-sectional area for the surrounding 1 mm case depth of altered chemistry is seen to be responsible for the difference in mechanical properties. As tension is a cross-sectional property the percentage difference for the same sample is seen to be different compared to flexure which is due to the maximum stress in the outer fibers. A favorable chemical change at the surface would affect flexure more than tension makes the material more brittle and less ductile. A more brittle material would show a good influence on the flexural strength. Flexible and ductile material would not benefit from a subsurface level structural change as its neutral axis would shift towards the tensile face during flexure tests, thereby reducing its strength. However, the tensile strength depends more on the cross-section of the case depth up to which a structural change is observed.

5. Fractographic analysis

Morphological studies of the polyethylene composite for different cutting conditions are shown in Fig. 8. Before the advanced cutting process, PE composite had limited porosity within the composite as seen in Fig.9 (a). Fiber debris and failure are more for conventional cut samples was the reason for low load-bearing capacity of the composite than advanced cutting. Fiber debonding is more between fiber and matrix for conventional cut samples. Fiber ductility is increased after laser cutting, the adhesion and debonding that occurred during conventional cutting are enhanced after laser cutting which increases the strength of the composite. Fiber fibrillation and debonding are less after advanced cutting. The surface morphology is less for AWJ samples.

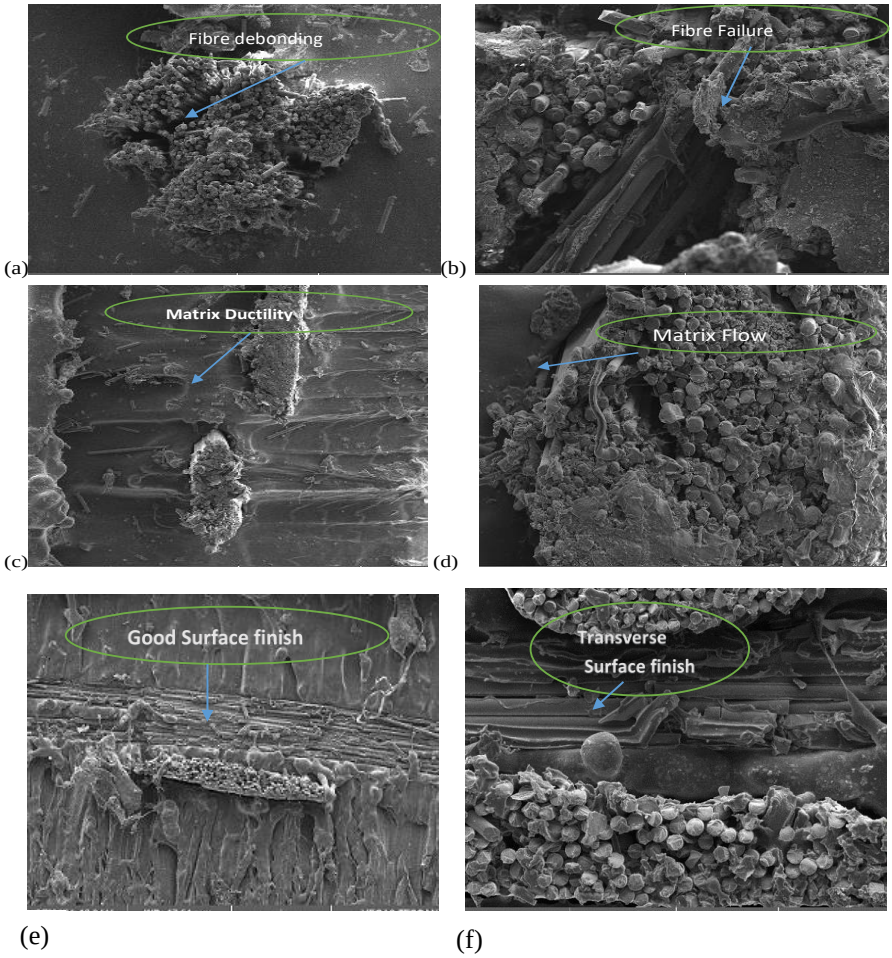

Fig.9. FESEM images of PE (a), (b) Conventional sample; (c),(d) laser-cut sample and (e), (f) AWJ sample.

The interface bonding between fiber and matrix is high, but the sample has become brittle compared to laser cutting after AWJ cutting as observed from Fig. 9(e) and Fig. 9(f), which affects the mechanical properties of the composite. The surface quality of the AWJ cut sample is good compared to conventional cut samples. The gap between the PE fiber and matrix keeps them from bonding well with each other in the laser approach. Fiber debris is highly visualized after conventional cutting. FESEM image of the Polyethylene SRC laminate after laser cutting concluded that carrying out the laser cutting process on Polyethylene SRC laminate samples improved the mechanical characteristics of the composite. Occasional fiber breakage is seen after laser cutting. PE is less ductile, but adhesion is good as shown in Fig.9 (c) and Fig. 9(d). Here, an interdiffusion of the matrix and fiber appears to occur due to the thermal effects associated with laser cutting. This will improve the tensile strength probably after laser cutting. Besides, the formation of stronger bonds as described earlier is also another reason for the improvement in strength due to laser cutting.

6. Impedance Analysis

EIS (Electron Impedance Spectroscopy) spectra of polyethylene SRC samples change with their chemical bonding and structural integrity as shown in Fig.10. In this experiment, the impedance of a conventionally cut sample decreases with frequency due to de-bonding of the layers of the laminate. Thermally-induced stresses developed in a laser-cut sample were higher and accompanied by appreciable initial values of impedance at lower frequencies compared to the AWJ cut samples or conventionally cut samples.

The de-bonding phenomenon was more noticeable in the conventionally cut samples than the AWJ cut samples. The laser-cut samples were least affected by impedance loss at lower frequencies as the thermal stresses led to the development of residual stresses in air cooling which resulted in lower levels of de-bonding as compared to the other two techniques. At higher frequencies, all the three types of cutting processes produced similar levels of impedance, closer to that of acoustic impedance of about 350 ohms in the air medium.

Another interesting characteristic measured from the EIS spectra of conventionally cut polyethylene sample is that the low-frequency impedance decreased from initial values in the range of 1000000.00 because of appreciable de-bonding of the matrix and fabric layers which were also observed in the SEM images as shown above. A decrease in phase angle with an increase in frequency is observed in Fig.10(c) for the laser cut and AWJ cut samples. Deterioration in the bonding and brittleness lead to an increase in phase angle as observed in the conventionally cut samples.

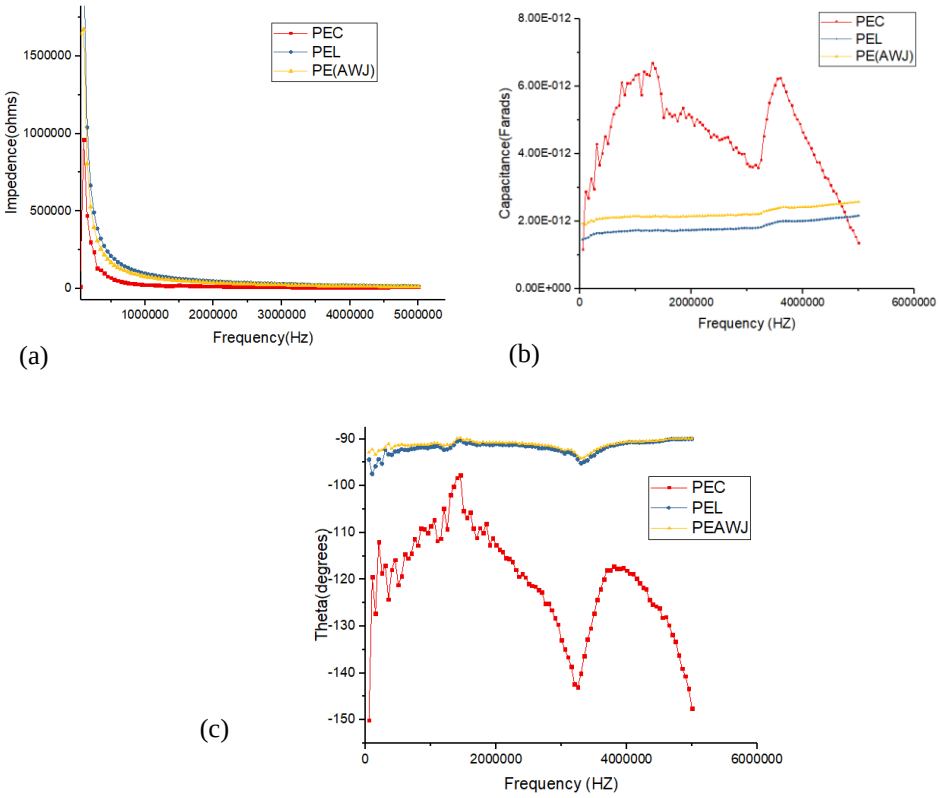

Fig.10**.** Electrical spectroscopy of Polyethylene samples for (a) impedance, (b) capacitance, and (c) phase angle

For laser cut and AWJ cut samples the magnitude of phase angle remains at about -100 to -90 degrees compared to conventionally cut samples because of the ductility, matrix flow and fewer de-bonding and delaminations [27].

7. Conclusion

The objective of the present work was the preparation and analysis of Polyethylene SRC laminate samples using different cutting methods. The strength of the sample depends strongly on the structural integrity which was confirmed experimentally. The influence of the advanced cutting on polyethylene SRC has been investigated experimentally. Weak aldehydes, acid groups and ethers are present initially transformed to alkenes, N-H bend after laser cutting. After AWJ cutting Alkoxy, acyl, N=C groups are formed which increases the strength of the composite. Fiber ductility is increased after laser cutting. The adhesion and de-bonding that occurred during conventional cutting were found to be reduced in laser machining and subsequent air cooling which increases the

strength of the composite. The tensile strength of all composites increased after advanced machining by about 20%. Degradation of the hydrates provides an enhancement in tensile strength of the composites. The flexural stress and load-bearing capacity of the laser samples were seen to be 42 MPa and 40 N respectively because of the formation of N-H Bend bonds and C-N bonds that also exhibited more brittleness and stiffness. Quality surface finish and low surface waviness were obtained after AWJ cutting compared to laser cutting. Finally, the forthcoming scope of works will explore to acknowledge the effects of the advanced machining for different processing temperate using the HOT compaction method. Drilling-induced damage for the respective processing temperature of Polypropylene SRC laminate samples with enhanced mechanical properties is also hereby proposed.

REFERENCES

[1] *Brzozowska-Stanuch, A., Rabiej, S., Fabia, J., & Nowak, J.* (2014). Changes in thermal properties of isotactic polypropylene with different additives during aging process. *Polimery*, *59*(4).

[2] *Baran, I., Cinar, K., Ersoy, N., Akkerman, R., & Hattel, J. H.* (2017). A review on the mechanical modeling of composite manufacturing processes. *Archives of computational methods in engineering*, *24*(2), 365-395.

[3] *Saha, D., Majumdar, M. K., Das, A. K., Chowdhury, A. M., & Ashaduzzaman, M.* (2019). Structural Nanocomposite Fabrication from Self-Assembled Choline Chloride Modified Kaolinite into Poly (Methylmethacrylate). *Journal of Composites Science*, *3*(3), 83.

[4] *Morgan, L & Weager, B & Hare, C & Bishop, G & Smith, G.* (2009). Self reinforced polymer composites: Coming of age. ICCM International Conferences on Composite Materials.

[5] *Kord, B., Ravanfar, P., & Ayrilmis, N.* (2017). Influence of organically modified nanoclay on thermal and combustion properties of bagasse reinforced HDPE nanocomposites. *Journal of Polymers and the Environment*, *25*(4), 1198-1207.

[6] *Dudarev, A., Volegov, K., & Kurzanov, G.* (2017). Rheonomic phenomenon shrinkage of holes drilled in fibreglass and carbon fibre-reinforced polymer composites. *Mechanics of Advanced Materials and Modern Processes*, *3*(1), 17.

[7] *Dhakal, H. N., Ismail, S. O., Ojo, S. O., Paggi, M., & Smith, J. R.* (2018). Abrasive water jet drilling of advanced sustainable bio-fibre-reinforced polymer/hybrid composites: a comprehensive analysis of machining-induced damage responses. *The International Journal of Advanced Manufacturing Technology*, *99*(9-12), 2833-2847.

[8] *Kartal, Fuat & Çetin, Muhammet & Gökkaya, H. & Yerlikaya, Zekeriya.* (2014). Optimization of Abrasive Water Jet Turning Parameters for Machining of Low Density Polyethylene Material Based on Experimental Design Method. International Polymer Processing. 29. 535-544. 10.3139/217.2925.

[9] *Mohammadi, F., Zinati, R. F., & Fattahi, A. M.* (2018). The effect of CNC and manual laser machining on electrical resistance of HDPE/MWCNT composite. *International Nano Letters*, *8*(2), 137-145.

[10] *Salama, A., Mativenga, P., & Li, L.* (2012). Tea CO2 laser machining of carbon fiber-reinforced polymer composites. In *International Congress on Applications of Lasers & Electro-Optics* (Vol. 2012, No. 1, pp. 302-308). LIA.

[11] *Datta, J., Kosiorek, P., & Włoch, M.* (2016). Effect of high loading of titanium dioxide particles on the morphology, mechanical and thermo-mechanical properties of the natural rubber-based composites. *Iranian Polymer Journal*, *25*(12), 1021-1035.

[12] *Xin, X., Liu, L., Liu, Y., & Leng, J.* Mechanical Models, Structures, and Applications of Shape-Memory Polymers and Their Composites. *Acta Mechanica Solida Sinica*, 1-31.

[13] *Das, D. K., Mishra, P. C., Singh, S., & Pattanaik, S.* (2014). Fabrication and heat treatment of ceramic-reinforced aluminium matrix composites-a review. *International Journal of Mechanical and Materials Engineering*, *9*(1), 6.

[14] *Barczewski, M., Matykiewicz, D., Krygier, A., Andrzejewski, J., & Skórczewska, K.* (2018). Characterization of poly (lactic acid) biocomposites filled with chestnut shell waste. *Journal of Material Cycles and Waste Management*, *20*(2), 914-924.

[15] *Cordin, M., Bechtold, T., & Pham, T.* (2018). Effect of fibre orientation on the mechanical properties of polypropylene–lyocell composites. *Cellulose*, *25*(12), 7197-7210.

[16] *Nizamuddin, S., Jadhav, A., Qureshi, S. S., Baloch, H. A., Siddiqui, M. T. H., Mubarak, N. M., & Ahamed, M. I.* (2019). Synthesis and characterization of polylactide/rice husk hydrochar composite. *Scientific reports*, *9*(1), 5445.

[17] *Hwang, Y. T., Kang, S. Y., Kim, D. H., & Kim, H. S.* (2019). The influence of consolidation temperature on in-plane and interlaminar mechanical properties of self-reinforced polypropylene composite. *Composite Structures*, *210*, 767-777.

[18] *Bahari, S. A., Grigsby, W., & Krause, A.* (2017). Thermal stability of processed PVC/bamboo blends: effect of compounding procedures. *European Journal of Wood and Wood Products*, *75*(2), 147-159.

[19] *Alomayri, T., Vickers, L., Shaikh, F. U., & Low, I. M.* (2014). Mechanical properties of cotton fabric reinforced geopolymer composites at 200–1000 C. *Journal of Advanced Ceramics*, *3*(3), 184-193.

[20] *Watanabe, R., Hagihara, H., & Sato, H.* (2018). Structure-property relationships of polypropylene-based nanocomposites obtained by dispersing mesoporous silica into hydroxyl-functionalized polypropylene. Part 1: toughness, stiffness and transparency. *Polymer Journal*, *50*(11), 1057.

[21] *Chouhan, H., Singh, D., Parmar, V., Kalyanasundaram, D., & Bhatnagar, N.* (2016). Laser machining of Kevlar fibre reinforced laminates–Effect of polyetherimide versus polypropylene matrix. *Composites Science and Technology*, *134*, 267-274.

[22] ASTM D638-10. Standard test method for tensile properties of plastics. West Conshohocken: ASTM International; 2010.

[23] ASTM D790-10. Standard test methods for flexural properties of unreinforced and reinforced plastics and electrical insulating materials. West Conshohocken: ASTM International; 2010.

[24] *Hejjaji, A., Singh, D., Kubher, S., Kalyanasundaram, D., & Gururaja, S.* (2016). Machining damage in FRPs: Laser versus conventional drilling. Composites Part A: Applied Science and Manufacturing, 82, 42-52.

[25] *Zhang, Z., Yao, X., Zhu, H., Hua, S., & Chen, Y.L.* (2009). Preparation and mechanical properties of polypropylene fiber reinforced calcined kaolin-fly ash based geopolymer. *Journal of Central South University of Technology*, *16*, 49-52.

[26] *Rajamohan, V., & Mathew, A. T.* (2019). Material and Mechanical Characterization of Multi-Functional Carbon Nanotube Reinforced Hybrid Composite Materials. *Experimental Techniques*, *43*(3), 301-314.

[27] *Davis, G., Rich, M.J., & Drzal, L.T.* (2004). Monitoring Moisture Uptake and Delamination in CFRP-Reinforced Concrete Structures with Electrochemical Impedance Sensors. *Journal of Non-destructive Evaluation*, *23*, 1-9.